Volume 1 | Number 1 | Jan 2013 | Pages 1–100

ChemComm

Chemical Communications
www.rsc.org/chemcomm

ROYAL SOCIETY OF CHEMISTRY

This is an *Accepted Manuscript*, which has been through the Royal Society of Chemistry peer review process and has been accepted for publication.

Accepted Manuscripts are published online shortly after acceptance, before technical editing, formatting and proof reading. Using this free service, authors can make their results available to the community, in citable form, before we publish the edited article. We will replace this *Accepted Manuscript* with the edited and formatted *Advance Article* as soon as it is available.

You can find more information about *Accepted Manuscripts* in the **Information for Authors**.

Please note that technical editing may introduce minor changes to the text and/or graphics, which may alter content. The journal's standard **Terms & Conditions** and the **Ethical guidelines** still apply. In no event shall the Royal Society of Chemistry be held responsible for any errors or omissions in this *Accepted Manuscript* or any consequences arising from the use of any information it contains.

Chem Commun

COMMUNICATION

Pyridine-copper (II) formates for the generation of high conductivity copper films at low temperatures

C. Paquet[a], T. Lacelle[a], B. Deore[a], A. J. Kell[a], X.Y. Liu[a], I. Korobkov[b], P. R.L. Malenfant[a]

Pyridine derivatives coordinated to copper (II) formates are shown to have lower decomposition temperatures than the alkylamine analogues. Using heating profiles compatible with low temperature substrates, deposited inks made from these compounds are transformed into copper traces with a resistivity value of 14 μΩ•cm when sintered at 135°C in < 5 minutes.

The production of low cost electronics relies on the ability to print conductive circuits using additive printing techniques on inexpensive plastic substrates.[1,2,3] It remains a challenge to formulate conductive inks that are inkjet, screen, flexographic, or gravure printable, while providing the required electrical and mechanical performance.[4-7] Although screen printable silver-flake conductive inks meet many of today's requirements and silver nanoparticles inks show promise due to their excellent electrical properties, few options exist for cost effective copper inks.[8-12] Copper coordination compounds are desirable ink materials as they are inexpensive, easy to prepare and process, compatible with a range of different printing methods and have excellent electrical properties.[13-19] For instance, copper formates coordinated to alkylamines convert to metallic copper under relatively mild conditions providing metallic traces with resistivity values as low as 5.0 μΩ•cm.[20] Unfortunately, the thermal sintering conditions typically used can cause polyethylene terephthalate (PET) to deform or simply alter its optical transmission thereby limiting their use with these substrates. In addition, sintering times on the order of 30 min further lessens their appeal, especially in a roll-to-roll process. Here we describe a new class of pyridine-copper (II) formate based inks capable of decomposing into copper films with low resistivity values at temperatures < 140°C and in under 5 min, thus making them more suitable for roll-to-roll printing on low temperature substrates.

Thermal decomposition of anhydrous copper (II) formate has been shown to occur near 200°C yielding Cu°, H_2 and CO_2 in a stepwise cation reduction reaction with copper (I) formate as an intermediate.[18] When copper (II) formate, $Cu(OOCH)_2$, is coordinated by alkylamines,

such as hexylamine and octylamine, the decomposition temperature is reduced to ~150°C.[13,22,23] Despite this significant decrease in decomposition temperature, the heating conditions required to convert these compounds into $Cu°$ remains too high for PET substrates under tension from a roll-to roll process. Pyridine derivatives once coordinated to $Cu(OOCH)_2$, form compounds that have significantly lower thermal decomposition temperatures than alkylamine derivatives. In addition, inks that combine pyridine-$Cu(OOCH)_2$ and alkylamine-$Cu(OOCH)_2$ generate copper films with high conductivity values while having low processing temperatures. To the best of our knowledge, this is the first report that demonstrates the potential of pyridine-copper complexes as metallic copper precursors with low temperature and rapid sintering. We compared two pyridine and two alkylamine derivatives of $Cu(OOCH)_2$ complexes, $L_2Cu(OOCH)_2$, where L=4-tert-butylpyridine, 3-butylpyridine, octylamine and 2-ethyl-1-hexylamine, named herein as tButPy, 3ButPy, *Octyl and EtHex* respectively. Although crystals of adequate quality for characterization by single-crystal X-ray diffraction were difficult to isolate, a crystal structure for *tButPy* was acquired showing that the copper atom bonds in a square planar geometry comprised of nitrogen atoms of the pyridine ligands and oxygen atoms from two formate molecules (see Figure 1). The formates have a slightly distorted *trans*-orientation. The two other formate oxygen atoms are weakly bonded to the copper in the normal direction to the square planar geometry of the CuO2N2 plane. Bond distances and angles are listed in the SI.

The thermal decomposition of these compounds heated under ambient conditions up to 150°C is illustrated in Figure 2. The images demonstrate how the blue copper (II) compounds decompose into metallic films. The two alkylamine-$Cu(OOCH)_2$ complexes, *Octyl* and *EtHex,* show visual signs of decomposition into copper at much higher temperatures (130°C) than the pyridine-$Cu(OOCH)_2$ complexes, *tButPy* and *3ButPy,* which decompose at approximately 115°C and 100°C, respectively.
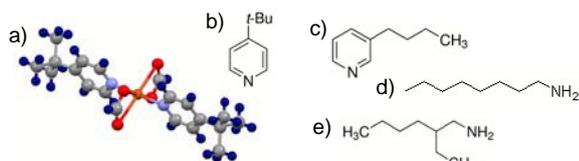
Fig. 1 a) Crystal structure of bis (tert-butylpyridine) copper (II) formate (*tButPy*). The molecular structure of the ligands b) 4-tert-butylpyridine, c) 3-butylpyridine and d) octylamine and e) 2-ethyl-1-hexylamine
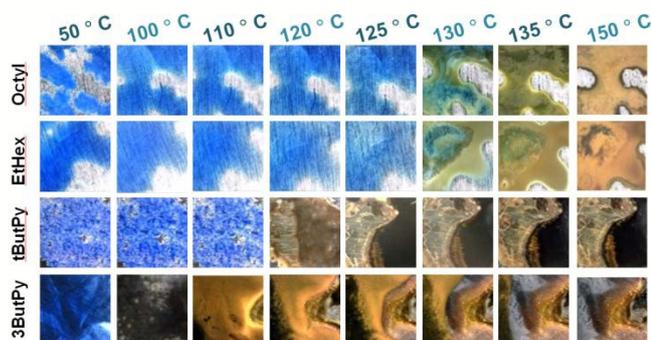

Fig. 2 Optical microscopy images of the copper (II) formate compounds heated to 150°C.

The thermal decomposition profile of these compounds was also monitored under inert conditions (Argon) by TGA-FTIR. Figure 3a compares the thermogravimetric analyses of the four compounds while the differential of the TGA curves (DTGA) in Figure 3b highlight the contrasting decomposition temperature of these compounds. The *tButPy* and *3ButPy* complexes decompose between 90-130°C and 75-120°C, respectively, whereas the mass loss of *Octyl* and *EtHex* complexes spans 100-155°C. The two peaks in mass loss point to a two-step reduction of copper complexes to metallic copper.
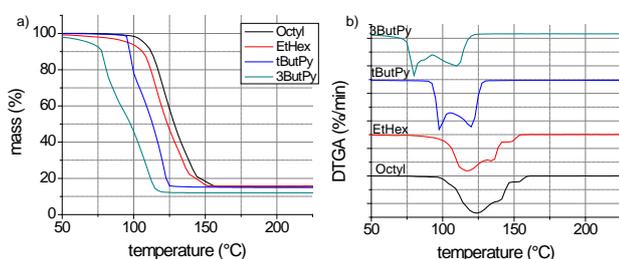

Fig. 3 a) The TGA and b) the DTGA of the amine- and pyridine-*Cu(OOCH)$_2$* complexes performed under Argon at 5°C/min.

Using TGA-FTIR, the volatile products of the decomposition reaction were identified as a function of temperature. An example of a 3D plot of the FTIR absorbance of the volatile products as a function of time and wavenumber can be found in the SI. The spectra show that the only products are CO_2 and the amine or pyridine ligand. This result indicates that the formate oxidation and copper reduction occur at the same time as the release of the amine or pyridine ligand, which implies that the activation barrier to reduction of copper (II) formate to Cu^o is governed by the presence of the amine or pyridine.

Furthermore, this result illustrates that the compounds decompose to metallic copper with no residue (*i.e.* CO_2, H2 and amines/pyridines are all volatile products). We found it instructive to compare the decomposition of the complexes by plotting the release of CO_2 and the amine ligand (as measured by the integrated FTIR absorbances at frequencies assigned to amine or CO_2 moieties) as a function of temperature as shown in Figure 4. The profiles show that the amines desorb concurrently with the release of CO_2, though the temperature range of pyridine release is broader than that of CO_2 and tails off at about 125°C for the pyridine complexes as opposed to a similar range for CO_2/amine release for the alkyl amine complexes. The CO2/amine release profile for the alkylamine complexes occur over the same range but tails off beyond 150°C. The CO_2 profiles are particularly informative as the release of CO_2 marks the onset of reduction from Cu^{2+} to Cu^{1+} and Cu^o defining a temperature window in which Cu^o forms, nucleates and grows into particles. This rate of nucleation and growth governs the size and size distribution of the particles. Based on the evolution profile of CO_2, the pyridine complexes decompose within a narrower temperature range than the alkylamine complexes, suggesting a more focused burst in nucleation leading to smaller particles with narrower size distribution. Scanning electron microscope (SEM) images of the films, shown in Figure 5a-c, confirm that the particles formed from *tButPy* have smaller diameters and narrower size distributions (26 +/- 6 nm) than particles made from *EtHex* (100 +/- 30 nm) and *Octyl* (240 +/- 60 nm).
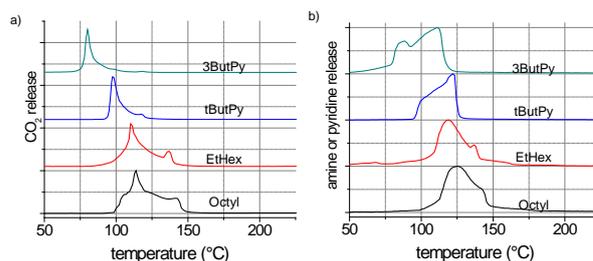

Fig. 4 The release of a) CO_2 and b) pyridine or alkylamines as measured from the integrated absorbance at 2200-2450cm^{-1} (CO2 vibrational mode), 1440-1480cm^{-1} or 1590-1610 cm^{-1} (methylene bending or ring stretching mode of amines or pyridine, respectively) as a function of temperature.
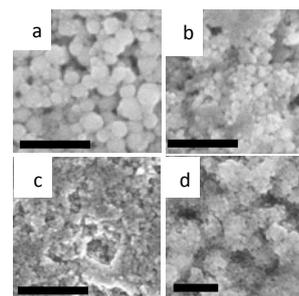

Fig. 5 SEM images of particles formed from a) *Octyl*, b) *EtHex* and c) *tButPy*; d) 60% *3ButPy*/40% *EtHex*. Scale bar: 1 μm.

Films made from the four complexes, prepared as described in the SI, were tape casted into 1 cm x 1 cm squares and heated using

convective heating under nitrogen (100 ppm oxygen) to temperatures ranging from 135 to 170°C for 4.5 minutes. Unlike the alkylamine derivatives, compounds *tButPy* and *3ButPy* decomposed into films with significant cracking with variable and high electrical resistance. As a result, electrical resistance measurements of these films were unreliable. Decreasing the rate of heating and lowering the sintering temperature failed to improve film quality. The cracks are likely formed as a result of the low surface tension of tert-butylpyridine and 3-butylpyridine, which generates capillary stresses in the particle-pyridine film. These capillary stresses lead to the formation of cracks in the film that follow the drying front.[24,25] To circumvent this shortcoming, inks containing a mixture of *EtHex* and *3ButPy* were prepared thus combining the good film forming properties of *EtHex* and the low decomposition temperature of *3ButPy*. *EtHex* and *3ButPy* were also chosen from the other compounds because they have good compatibility with each other and good solubility in organic solvents due to their branched structure and long alkyl side chain. An optimal weight fraction of *3ButPy* (e.g. *3ButPy/3ButPy+EtHex*) was determined by sintering at 170°C to ensure that all samples were fully sintered. Figure 6a shows that the resistivity of the films gradually decreases as the fraction of *3ButPy* increases. A minimum resistivity of 6.5 μΩ·cm was achieved with 60% *3ButPy (see also Table 1)*. In Figure 6b, we compare the resistivity values of pure *EtHex* complex (red circles) to a blend of 60% 3ButPy (black squares) in order to assess their performance as a function of temperature. The resistivity values decrease as the sintering temperature is increased to 170°C in both cases but increased at 185°C concurrent with increases in the error in the resistivity values and the formation of a blackened surface. Therefore, above a sintering temperature of 170°C, oxidation plays an increasingly important role in degrading the electrical characteristics of the films. At 170°C, the *3ButPy/EtHex* ink outperformed the pure *EtHex* ink in terms of resistivity and at 135°C produced films with a resistivity of 13.9 μΩ·cm, whereas the *EtHex* derived traces were non-conductive. Figure 5d illustrates the morphology of the film made from 60% 3ButPy. Films prepared on PET substrates showed similar results and did not show signs of deformation at 135°C (see SI).

Table 1. The substrate compatibility of *EtHex* and *3ButPy/EtHex* inks based on resistivity values of films sintered for 4.5 minutes at various temperatures. PEN = polyethylene naphthalate.

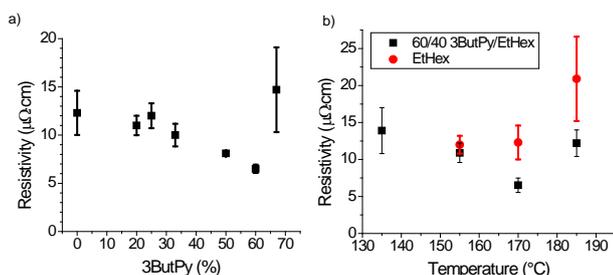| Ink	Sintering temperature (°C)	Resistivity (μΩ·cm)	Substrate compatibility
EtHex	135	non conductive	-
	170	12.3	PEN, Kapton
3ButPy/EtHex (60% 3ButPy)	135	13.9	PET
	170	6.5	PEN, Kapton

Fig. 6 a) Resistivity as a function of the weight fraction of *3ButPy* to *EtHex* after heating to 170°C. B) Resistivity of copper films as a function of the maximum sintering temperature for *EtHex* (red circles) and the blend containing 60% *3ButPy* (black squares).

Conclusions

In conclusion, pyridine derivatives coordinated to copper formate have lower decomposition temperatures than their alkylamine counterparts. The 3-butyl-pyridine ligand, coordinated to copper (II) formate, initiates decomposition near 80°C, ~30°C lower than alkylamine-$Cu(OOCH)_2$ derivatives. Although on its own bis(3-butyl-pyridine) copper (II) formate has poor film forming properties, the complex can be combined with bis(2-ethyl-1-hexylamine) copper (II) formate to yield an ink with good film forming properties, short sintering times and low decomposition temperatures, making it more suitable for roll-to-roll printing on low temperature substrates.

Notes and references

1   J. Perelaer, P. J. Smith, D. Mager, D. Soltman, S.K. Volkman, V. Subramanian, J.G. Korvink, U.S. Schubert, *J. Mater. Chem.* 2010, **20**, 8446.

2   B. Kang, W.H. Lee, K. Cho, *ACS Appl. Mater. Interfaces* 2013, **5**, 2302.

3   H. Kang, H. Park, Y. Park, M. Jung, B.C. Kim, G. Wallace, G. Cho, *Sci. Rep.* 2014, **4**, 5387.

4   K.-J. Baeg, M. Caironi, Y.,-Y. Noh, *Adv. Mater.* 2013, **25**, 4210.

5   A. Kamyshny, J. Steinke, S. Magdassi, *TOAPJ* **2011**, **4**, 19.

6   J. Noh, M. Jung, Y. Jung, C. Yeom, M. Pyo, G. Cho, *Proc. IEEE*, **2015**, *103*, 554-566

7   S. Norita, D. Kumaki, Y. Kobayashi, T. Sato, K. Fukuda, S. Tokito, *Org. Electron.* 2015, **25**, 131.

8   K.-Y. Shin, J.S. Lee, J.-Y. Hong, J. Jang, J. *Chem. Commun.* 2014, **50**, 3093.

9   S. Bhagat, N.D. Theodore, S. Chenna, T. Alford, *Appl. Phys. Express*

10 H.-J. Hwang, W.-H. Chung, H.-S. Kim, *Nanotechnology* 2012, **23**, 485205.

11 K. Woo, C. Bae, Y. Jeong, D. Kim, J. Moon, *J. Mater. Chem.* 2010, **20**, 3877.

12 C. Paquet, R. James, A. J. Kell, O. Mozenson, J. Ferrigno, S. Lafreniere, P. R. L. Malenfant *Org. Electron.* 2014, *15, 1836*.

13 A. Yabuki, N. Arriffin, M. Yanase, *Thin Solid Films* 2011, **519**, 6530.

ChemComm Accepted Manuscript

14 R. Dharamada, M. Jha, D.A. Amos, T. Duffel, *ACS Appl. Mater Interfaces*, 2013, **5**, 13227.

15 T. Araki, T. Sugahara, J. Jiu, S. Nagao, M. Nogi, H. Koga, H. Uchida, K. Shinozaki, K. Suganuma, *Langmuir* 2013, **29**, 11192.

16 Y.-H. Choi, J. Lee, S. J. Kim, D.-H. Yeon, Y. Byun, *J. Mater. Chem.* 2012, **22**, 3624.

17 I. Kim, Y. Kim, K. Woo, E.-H. Ryu, K.-Y. Yon, G. Cao, J. Moon, *RSC Adv.* 2013, **3**, 15169.

18 D.-H. Shin, S. Woo, H. Yem, M. Cha, S. Cho, M. Kang, S. Jeong, Y. Kim, K. Kang, Y. Piao, *ACS Appl. Mater. Interfaces* 2014, **6**, 3312.

19 D. Adner, F. M. Wolf, S. Möckel, J. Perelaer, U. S. Schubert, H. Lang, *Thin Solid Films* 2014, **565**, 143.

20 A. Yabuki, S. Tanaka, *Mater. Res. Bull.* 2012**, 47,** 4107.

21 M. A. Mohamed, A. K. Galwey, S. A. Halawy, *Thermochim. Acta* 2004, **411**, 13.

22 S. J. Kim, J. Lee, Y.-H. Choi, D.-H. Yeon, Y. Byun, *Thin Solid Films* 2012, **520**, 2731.

23 M. A. Bernard, A. Busnot, F. Busnot, J. F. Le Querler, *Thermochim. Acta* 1985, **86**, 33.

24 W. Man, W. Russel, *Phys. Rev. Lett.* 2008, **100**, 198302.

25 K. Singh, M. Tirumkudulu, *Phys. Rev. Lett.* 2007, **98**, 218302.

ChemComm Accepted Manuscript